PHILOSOPHICAL TRANSACTIONS OF THE ROYAL SOCIETY A MATHEMATICAL, PHYSICAL & ENGINEERING SCIENCES

Numerical Modelling of Tide-Surge Interaction in the Bay of Bengal

B. Johns, A. D. Rao, S. K. Dube and P. C. Sinha

Phil. Trans. R. Soc. Lond. A 1985 **313**, 507-535
doi: 10.1098/rsta.1985.0002

Phil. Trans. R. Soc. Lond. A **313**, 507–535 (1985) [507]
Printed in Great Britain

NUMERICAL MODELLING OF TIDE–SURGE INTERACTION IN THE BAY OF BENGAL

By B. Johns,[1] A. D. Rao,[2] S. K. Dube[2] and P. C. Sinha[2]

[1] *Department of Meteorology, University of Reading, Reading RG6 2AU, U.K.*
[2] *Centre for Atmospheric Sciences, Indian Institute of Technology, New Delhi, India*

(*Communicated by Sir James Lighthill, F.R.S. – Received* 20 *July* 1984)

CONTENTS

	PAGE
1. Introduction	508
2. Description of the models	510
3. Generation of tides and verification of model B	516
4. The tide in the upper Bay of Bengal on 3 June 1982	517
5. The surge response along the Orissa coast on 3 June 1982	521
6. Tide–surge interaction along the Orissa coast on 3 June 1982	524
7. The surge response along the Andhra coast between 18–20 November 1977	530
8. Tide–surge interaction along the Andhra coast	532
9. Concluding remarks	534
References	535

Numerical models are described for the evaluation of the interaction between tide and surge in the Bay of Bengal. The models are used to simulate the combined tidal and surge response on 3 June 1982 along the Orissa coast of India when the landfall of a tropical cyclone led to severe inland flooding. This is one of the few events for which a reliable tide-gauge reading is available and this enables a direct comparison to be made between the model predictions and the observationally determined sea-surface elevation anomaly. The comparison, although only utilizing limited observational data, appears sufficiently good for us to assert that the principal features of the surge response are correctly reproduced.

A model simulation is also made of the surge that occurred along the Andhra coast of India during the period 18–20 November 1977 when there was heavy coastal inundation. Although tide-gauge readings are not available for this event, the predicted surge response agrees well with indirect estimates of the maximum sea-surface level and eyewitness accounts of inland flooding.

The principal requirement for the operational use of these models is the availability of accurate data on the surface wind field together with a reliable forecast of the track to be followed by the tropical cyclone.

1. Introduction

Flierl & Robinson (1972) have documented many cases where the occurrence of abnormally high sea-surface levels in the Bay of Bengal has led to coastal flooding and inundation. The genesis of these events is to be found in the combined effect of the astronomical tide and a surge generated by a tropical cyclone. The principal component is the surge but, depending on the relative phase of the two processes, the sea-surface elevation may either be increased above, or decreased below its pure surge value. The mutual interaction is, however, nonlinear and the dynamics of both processes must be considered simultaneously.

Many analyses of surge generation by hurricanes, typhoons and tropical cyclones have now been made. Particular mention is made here of the numerical modelling of these phenomena by Jelesnianski (1965, 1966, 1967), Miyazaki *et al.* (1961) and Das *et al.* (1974). More recently, Johns *et al.* (1981, 1982, 1983*a*, *b*) have developed several numerical models for application along the east coast of India. A fully nonlinear model to analyse tide–surge interaction in the Bay of Bengal has been described and applied to the coastal waters off Bangladesh by Johns & Ali (1980).

The general procedure followed in the modelling of tide–surge interaction is to begin by generating the co-oscillating tide in a semi-enclosed basin by prescribing the temporal variation of the sea-surface elevation along the open boundary. The value of this is supposed known from observations of the tidal state in the adjacent ocean. The pure tidal solution developed in the basin then provides the initial dynamical conditions for the storm surge simulation with tidal forcing along the open-sea boundary continuing during the integration. This method has been successfully applied in studies of the tide–surge interaction in the North Sea (see, for example, Banks 1974) but its practical application in the Bay of Bengal is hampered by the absence of adequate tidal data along the boundary separating the Bay from the northern Indian Ocean.

The principal purpose of the present work is to evaluate the tide–surge interaction during the event of 3 June 1982 when part of the Orissa coast of India was inundated by a severe storm-generated surge. This was one of the few surge events for which any reliable tide-gauge data are available and this enables us to appraise the ability of the numerical model to reproduce the observed maximum sea-surface elevation. Unfortunately, a continuous record of tide-gauge measurements throughout the duration of the event is not available to us. Until there is a continuous monitoring by an extended network of reliable gauges along the east coast of India, however, we are unlikely to have access to any better data describing an actual surge event. Therefore, the best we can do is to make the most effective use of the limited data that are available for the Orissa surge.

An examination is also made in this paper of the surge event affecting Divi Island off the Andhra coast of India on 19 November 1977. The precise tidal conditions existing there during this period are not available in documented form and there are no tide-gauge readings of maximum sea-surface levels. Our purpose is to re-evaluate the pure surge response and to interpret this in the light of eyewitness accounts of flooding along the Andhra coast. We also perform a tide–surge interaction experiment in which the phase of the tide is chosen to yield a maximal interactive effect with the surge dynamics. The experiment enables us to estimate the contribution made by the tidal response in the generation of high sea-surface levels along part of the Andhra coast.

The basic model used is that described by Johns *et al.* (1981) in which the western and eastern

coasts of the Bay of Bengal are represented in terms of a curvilinear boundary treatment. The northern extremity of the region, which includes the orographically complicated Ganges Delta, is represented in the model by a southward facing coastal boundary. Therefore, interactions between the Bay and the complex river systems at its head are not incorporated. The east coast of India, which is our principal region of interest, is realistically modelled in this scheme. The Andaman Sea and the complicated west coasts of Burma and Thailand are not represented in detail. This basic model has a single open-sea boundary at the latitude at which it communicates with the northern Indian Ocean. The prescription of tidal forcing along this boundary leads to the generation of the co-oscillating tide in the Bay. Additionally, the distance of the boundary from the headbay and the northeast coast of India is hopefully such as to minimize the effect of uncertain tidal forcing data on the response in the regions of interest. However, this basic scheme is not in itself adequate for our proposed simulations. The failure to include any representation of the Ganges Delta is likely to misrepresent both the tidal and surge responses in the headbay. A shortcoming to be found in the curvilinear boundary representation is its inability to represent coastal orographical detail. Accordingly, we have applied the basic scheme as a parent model. Appropriate high resolution models are nested within this to record fine orographical detail in the regions of principal interest. This is particularly important for the headbay region where the nested model includes a dynamical representation of the major rivers comprising the Ganges Delta. The inclusion of these allows a mutual interaction between the dynamics in the Bay and those in the Delta. We have also developed a nested model to examine the tidal and surge response along the Andhra coast.

A procedural problem in the use of nested models is encountered in the linking of these to the parent model. There are two essentially different ways in which this may be done. In the first, the interaction between the parent and nested models is one-way. This implies that the parent model drives the nested model but the response in the nested model does not affect that in the parent model. In the second method, the interaction is two-way, implying that the response in either model affects that in the other. We adopt the former method. There still remains, however, the question of the appropriate boundary conditions through which the response in the nested model is driven by that in the parent model. This can be done by utilizing the predicted elevations from the parent model and applying these as input conditions around the boundary of the nested model. Alternatively, the nested model can be driven by applying approximate radiation conditions around the boundary based on the response calculated in the parent model. The first method does not imply any linearization and is probably more appropriate in shallow water. The second is strictly valid only in deep water where nonlinearity and bottom friction are of secondary importance and is then probably superior to the first. In this paper, both methods are used, the choice depending on the particular circumstances of the application.

In Nature, the surge component in the sea-surface response is generated by contributions from both barometric and wind-stress forcing. The precise details of this forcing depend on the structure of the cyclone and vary from one event to another. One of the more simple approaches used has been to prescribe the atmospheric pressure distribution in the cyclone in terms of observationally determined parameters (see, for example, Reid *et al.* 1977). By assuming, for example, that the corresponding wind distribution satisfies a gradient balance, an empirical formula may be used to estimate the surface wind-stress in terms of the wind speed. Barometric and wind-stress forcing are then readily incorporated into a model calculation. However, the

PHILOSOPHICAL TRANSACTIONS OF THE ROYAL SOCIETY A MATHEMATICAL, PHYSICAL & ENGINEERING SCIENCES

surface wind-speed thus derived from a simple postulated pressure distribution rarely correlates with values obtained by direct measurement. Accordingly, an alternative approach (Jelesnianski 1965) has been to prescribe directly the wind speed by an empirical formula. This appears rather more satisfactory than the former approach in so far as the representation of the wind-stress forcing is concerned. Nevertheless, the problem of the corresponding barometric forcing is still outstanding. In principle, this could be deduced from the assumed wind-speed distribution by consideration of a prescribed dynamical balance in the cyclone. However, the resulting pressure distribution is naturally dependent upon the form of the postulated balance in the atmospheric boundary layer. On the other hand, experience shows that, in shallow water at least, the contribution from wind-stress forcing dominates that from barometric forcing (Jelesnianski 1965). In view of these circumstances, we have decided to omit the direct inclusion of barometric forcing and to regard its effect as being equivalent to the application of a corrective adjustment in the predicted sea-surface level amounting to a rise of about 1 cm for a 1 mbar† drop in atmospheric pressure. Accordingly, the forcing in the models described in this paper derives solely from the applied surface wind stress. Until more reliable and relevant data are available concerning the structure of Bay of Bengal cyclones, this procedure appears satisfactory.

2. Description of the models

We consider two types of model that are then combined into a unified computational scheme. The major component consists of the basic curvilinear model for the Bay of Bengal (referred to as model A), described by Johns *et al.* (1981). The second component is a nested, and more conventional, high resolution stair-step model of the type described, for example, by Heaps (1969).

The curvature of the earth's surface is neglected and all conditions are referred to a system of plane Cartesian coordinates. With the origin, O, located within the equilibrium level of the sea-surface and at the southwestern extremity of model A, Ox points towards the east, Oy towards the north and Oz is directed vertically upwards. The displaced position of the sea surface is given by $z = \zeta(x, y, t)$ and the position of the sea floor by $z = -h(x, y)$. An open-sea boundary at $y = 0$ corresponds approximately to latitude 6° N. A northern coastal boundary is situated at $y = L$ (taken as 1800 km) and western and eastern coastlines correspond respectively to $x = b_1(y)$ and $x = b_2(y)$. The coastal boundary configuration in model A is delineated in figure 1.

Conventional depth-averaged equations of motion are used in which the depth-averaged components of velocity, u and v, satisfy

$$\frac{\partial u}{\partial t}+u\frac{\partial u}{\partial x}+v\frac{\partial u}{\partial y}-fv=-g\frac{\partial \zeta}{\partial x}+\frac{1}{H}\frac{\tau_x^{\zeta}}{\rho}-\frac{ku}{H}(u^2+v^2)^{\frac{1}{2}} \tag{1}$$

and

$$\frac{\partial v}{\partial t}+u\frac{\partial v}{\partial x}+v\frac{\partial v}{\partial y}+fu=-g\frac{\partial \zeta}{\partial y}+\frac{1}{H}\frac{\tau_y^{\zeta}}{\rho}-\frac{kv}{H}(u^2+v^2)^{\frac{1}{2}}. \tag{2}$$

In (1) and (2), f denotes the Coriolis parameter, the pressure is taken as hydrostatic and the direct effect of the astronomical tide-generating forces is omitted. In accordance with our comments in §1, we have also omitted those terms representing the effect of barometric forcing.

† 1 mbar = 10^2 Pa.

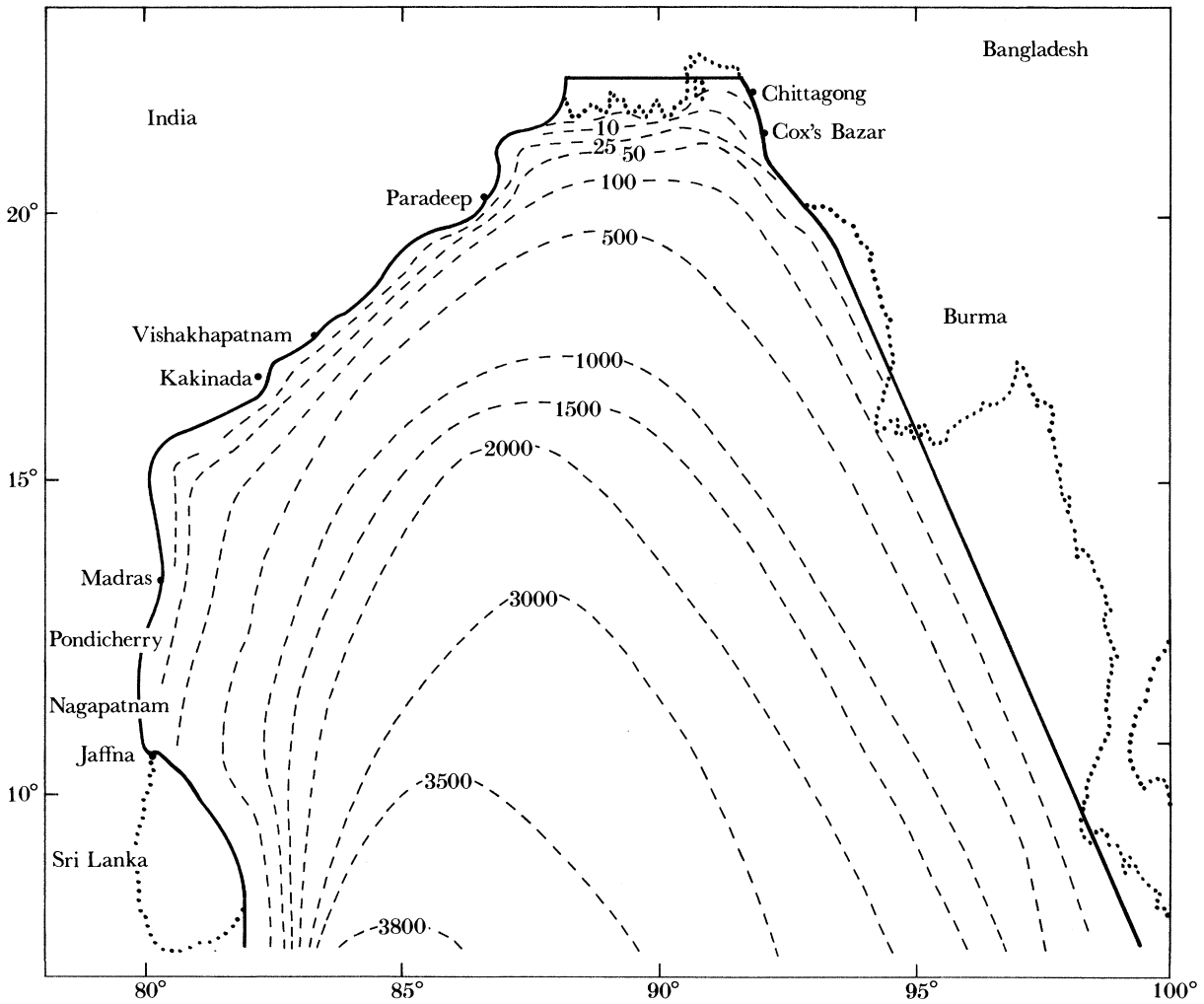

FIGURE 1. The coastal configuration in model A and the isobaths of the model bathymetry. The numbers refer to depths in metres.

The sole explicitly included forcing agency is the applied surface wind stress $(\tau_x^\zeta, \tau_y^\zeta)$. Bottom friction is parametrized in terms of a conventional quadratic stress law with the friction coefficient, k, taken as uniform and equal to 0.0026. The density of the water, ρ, is assumed uniform and H is the total depth, $(\zeta+h)$.

The equation of continuity in vertically integrated form is

$$\frac{\partial \zeta}{\partial t}+\frac{\partial}{\partial x}(Hu)+\frac{\partial}{\partial y}(Hv)=0. \tag{3}$$

Boundary conditions along the coastlines require that the normal component of velocity be zero. In terms of the general formulation of model A, these lead to

$$u-vb_1'(y)=0 \quad \text{at} \quad x=b_1(y), \tag{4}$$

$$u-vb_2'(y)=0 \quad \text{at} \quad x=b_2(y) \tag{5}$$

and

$$v=0 \quad \text{at} \quad y=L. \tag{6}$$

At the southern open-sea boundary of model A we use a generalization of the linearized radiation condition successfully applied by Johns *et al.* (1981). As well as allowing for the approximate outward radiation of an internally generated response from the analysis region, it also communicates the tides of the northern Indian Ocean into the Bay of Bengal. The condition has the form

$$v + (g/h)^{\frac{1}{2}}\zeta = 2a(g/h)^{\frac{1}{2}} \sin\{(2\pi t/T) + \phi\} \quad \text{at} \quad y = 0. \tag{7}$$

In (7), a and ϕ denote respectively the prescribed amplitude and phase of the tidal forcing and T is the period of the tidal constituent under consideration.

If the tidal response entering the Bay crosses $y = 0$ in the form of a progressive wave with its crest parallel to $y = 0$, then $v = (g/h)^{\frac{1}{2}}\zeta$ and (7) reduces to

$$\zeta = a \sin\{(2\pi t/T) + \phi\} \quad \text{at} \quad y = 0. \tag{8}$$

In this case, a and ϕ correspond to the amplitude and phase of the tidal elevation along $y = 0$. A consequence of applying (7) rather than (8) is that the values of neither ζ nor v are separately prescribed along the open-sea boundary of model A. Thus, during the solution process, the boundary values of both ζ and v may correlatively adjust subject only to (7). We anticipate that such a solution procedure, which is based on prescribing conditions on an incoming characteristic, will be superior to one using (8), especially if $y = 0$ should coincide with a nodal line. Further generalization of (7) to a discrete spectrum of tidal constituents follows without difficulty.

High resolution stair-step models are nested within model A so as to represent more fully the orographical detail of the headbay region and the Andhra coast of India. For the headbay, the nested model is referred to as model B and the stair-step boundary configuration is delineated in figure 2. In contrast with the parent model A, the northern boundary of model B does not consist of a continuous vertical wall. Instead, one-dimensional dynamical models have been included to represent some of the rivers entering the head of the Bay of Bengal. The southernmost limit of model B consists of an open-sea boundary along latitude 19° 33′ N where elevation values are prescribed. These are determined from the response in model A. An important feature of the scheme is that the response in model A is independent of that in model B. On the other hand, the response in model B is dependent on that generated in model A. Indeed, we find that the results from model A become increasingly unrealistic in the region of the Ganges Delta owing to the omission of any representation of the complex river system. Model B is superior in this respect as the representation of the rivers, although crude, avoids a complete reflection of the response at $y = L$ and the local development of unrealistically high sea-surface elevations.

In model B, the east–west separation distance between points at which the elevation is computed is approximately 17.6 km. The north–south distance between computational points is approximately 19.8 km. The grid-point arrangement is staggered in such a way that ζ is computed at the centre of a grid cell while u and v are computed at the mid-points of its y-directed and x-directed sides respectively. The vanishing of the normal component of velocity at a coastline is then readily achieved by an appropriate stair-step representation of the boundary.

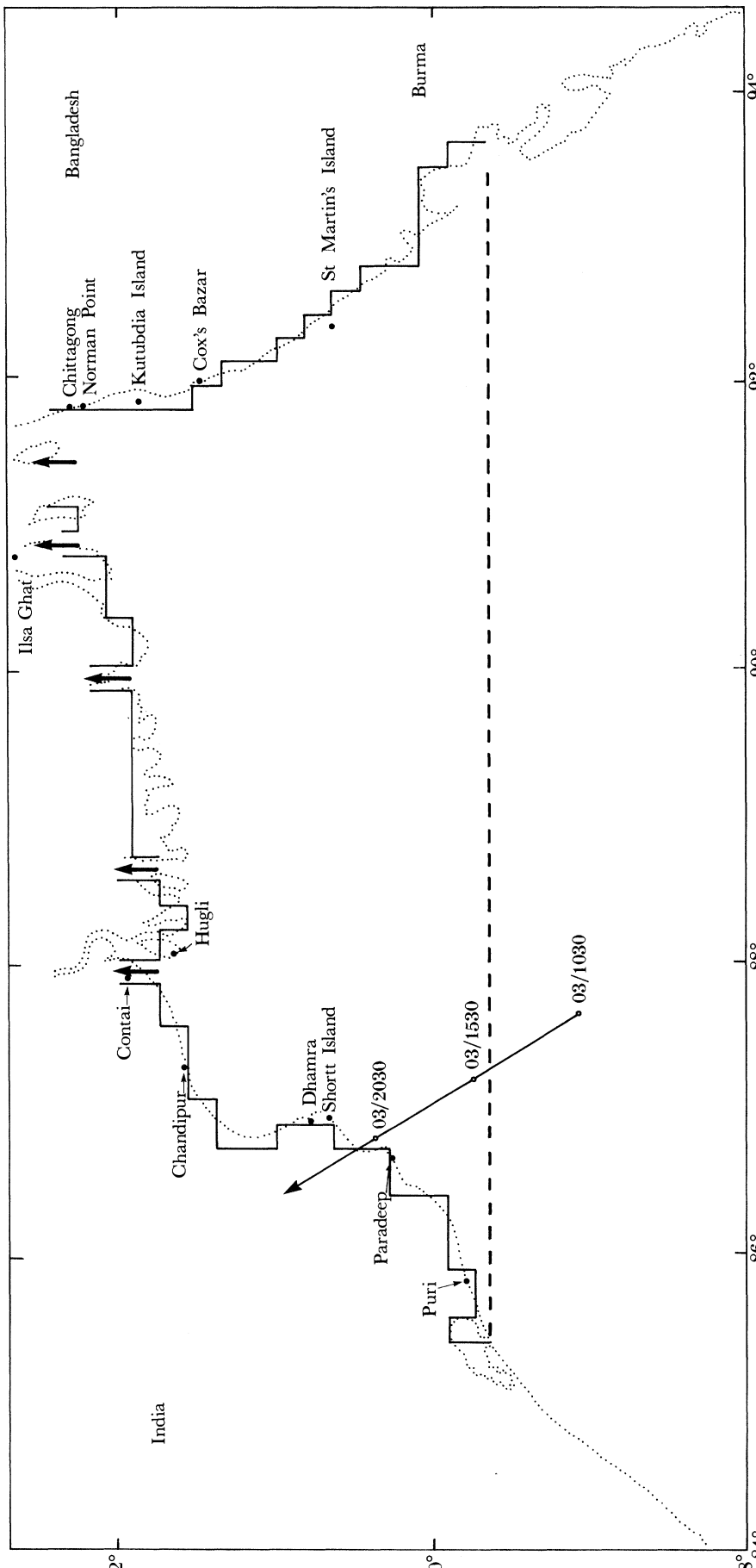

FIGURE 2. The coastal configuration in model B and the idealized track of the Orissa cyclone. The numbers on this track refer to the times (in I.s.t.) at which the centre of the cyclone passed through the marked positions on 3 June 1982.

PHILOSOPHICAL TRANSACTIONS OF THE ROYAL SOCIETY A MATHEMATICAL, PHYSICAL & ENGINEERING SCIENCES

Conditions in each of the rivers satisfy equations of the form

$$\frac{\partial v}{\partial t}+v\frac{\partial v}{\partial y}=-g\frac{\partial \zeta}{\partial y}-\frac{kv|v|}{H} \tag{9}$$

and

$$b\frac{\partial \zeta}{\partial t}+\frac{\partial}{\partial y}(bHv)=0. \tag{10}$$

Thus, in the dynamical equation (9), we omit the effect of wind-stress forcing in the rivers. At the point of entry into model B, the elevation and momentum flux are made continuous. In the continuity equation (10), b denotes the local breadth of the river. At the river's point of communication with model B, the mass flux is made continuous. Juncture conditions of a similar kind have been described by Johns & Ali (1980). It is noteworthy that the resulting interaction between the rivers and model B is two-way because the dynamical response in either may affect that in the other.

Each of the rivers is taken to have a length of 200 km with no mass flux of water through its head. Each river has a uniform breadth of 18 km except the Meghna (in the extreme east), which has a breadth of 54 km. The depth of each river is uniform and equal to that at its point of communication with model B. The distance between computational elevation points is taken as 20 km.

The second of the nested stair-step models (referred to as model C) is designed to provide high resolution in surge experiments along the Andhra coast of India. The boundary configuration of model C is delineated in figure 3. It communicates with model A across two open-sea boundaries along which linearized radiation conditions are prescribed by using an input derived from the computed response in model A. It has been our experience that the prescription of the elevation along more than one open-sea boundary may lead to computational problems that are avoided by using radiation conditions. Accordingly, along the north–south boundary, we require that

$$u-(g/h)^{\frac{1}{2}}\zeta=-2(g/h)^{\frac{1}{2}}\zeta_{\mathrm{B}}, \tag{11}$$

and along the east–west boundary

$$v+(g/h)^{\frac{1}{2}}\zeta=2(g/h)^{\frac{1}{2}}\zeta_{\mathrm{B}}. \tag{12}$$

In (11) and (12), ζ_{B} denotes the interpolated sea-surface elevation along the open-sea boundaries as derived from model A. These conditions are approximations to the requirement that a response generated internally in model C will be radiated across the boundaries and out of the computational domain. If there is no such response (in which case model C would respond identically to model A in the region of overlap) then (11) and (12) are equivalent to the condition $\zeta=\zeta_{\mathrm{B}}$ along the boundaries.

The computational grid for model C is of the same type as that for model B with an east–west grid increment of 10.4 km and a north–south increment of 10.75 km.

An important part of the design of a model to simulate tides and surges is the correct representation of the bathymetry. The obvious way of doing this is to extract interpolated grid-point values of the depth from a hydrographic chart. This is, however, extremely laborious and, with our present combination of parent and nested models, it is necessary that the depths in model A be consistent with those in models B and C. By using the fact that the coordinate systems in each of our models have a common origin, the equilibrium depth is conveniently

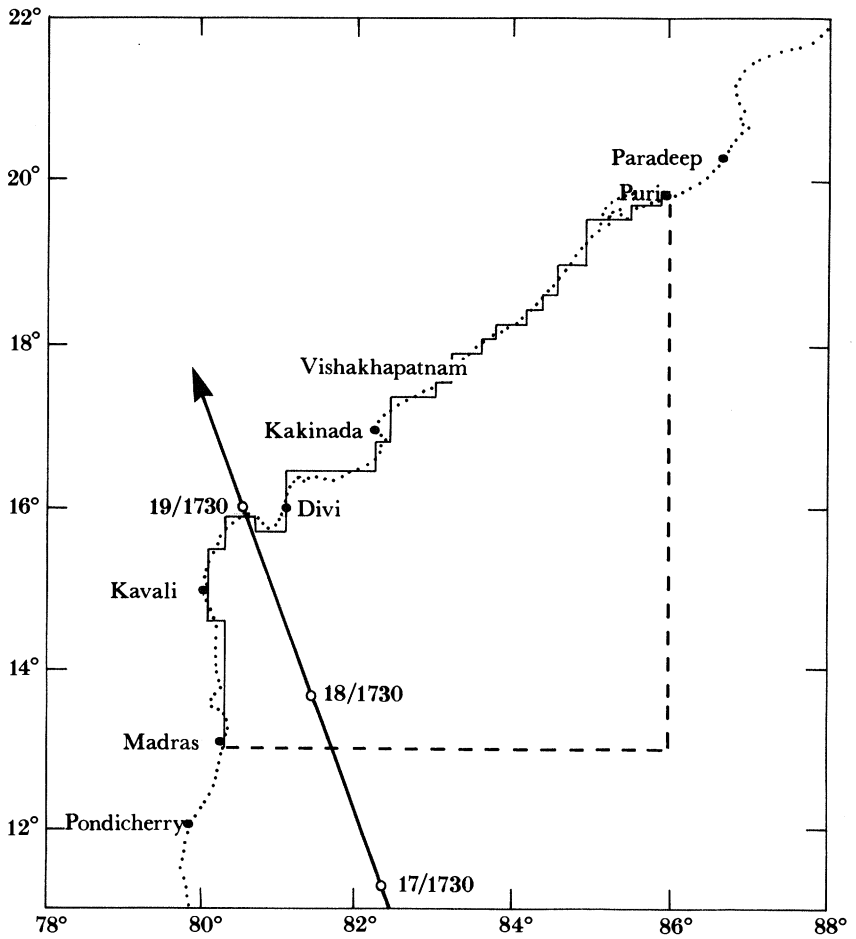

FIGURE 3. The coastal configuration in model C and the idealized track of the Andhra cyclone. The numbers on this track refer to the times at which the centre of the cyclone passed through the marked positions between 17–19 November 1977.

represented as a function of x and y. This is done by a scheme of interpolation based on distance weighting in which

$$h(x, y) = \sum_{k=1}^{N} h_k\, b_k(x, y) \Big/ \sum_{k=1}^{N} b_k(x, y). \tag{13}$$

In (13), the h_k are spot depths at the points (x_k, y_k) which are read from a hydrographic chart. The b_k are base functions defined by

$$b_k(x, y) = \exp\left[-(\mu_k/L)^2\{(x-x_k)^2 + (y-y_k)^2\}\right], \tag{14}$$

where μ_k is a numerical factor determining the radius of influence of the spot depth h_k. N denotes the number of spot depths used in the bathymetric representation. Then, with suitable choices for the h_k and μ_k, we are able to represent a smoothed version of the bathymetry to any desired degree of accuracy. In our applications, we find that the bathymetry in model A, where this overlaps with model B, is well represented by taking $N = 41$ and $\mu_k = 286$. In the remaining area covered by model A, we take $N = 68$ and $\mu_k = 1395$. The bathymetry in models B and C is, by definition, consistent with that in model A. The 109 spot depths are read from British

Admiralty hydrographic charts and our selection of these leads to a realistic representation of the overall bathymetry. The corresponding isobaths are shown in figure 1 and, in accordance with the hydrographic charts, the equilibrium depths are seen to vary between 5 m in the mouth of the river Meghna and 3800 m to the east of Sri Lanka.

3. Generation of tides and verification of model B

The paucity of data on surges generated along the Orissa coast of India is such that a direct verification of model B for surge prediction is not possible. However, because some form of verification is necessary, we have used coastal data available for the pure M_2 tidal response in the Bay of Bengal. If a comparison of the computed and observed tidal response is satisfactory, we would feel justified in asserting that the dynamical processes are correctly represented in the model.

A severe handicap encountered in the verification procedure is the uncertainty concerning values of the parameters in the tidal forcing along the open-sea boundary of model A. If values of a and ϕ in (7) were known with precision along this boundary (which would necessitate a knowledge of both ζ and v), there would be no problem in integrating the model equations ahead in time subject to the prescribed forcing along $y = 0$. From an initial state of rest, the transient response would be gradually dissipated by friction and also radiated out of the computational domain. Thereafter, an oscillatory response would remain in the Bay corresponding to the tidal constituent with period T. Unfortunately, precise values of a and ϕ are not available. Therefore, we have had to resort to numerical experimentation and a series of tests to ascertain values for the forcing parameters that produce the correct order of magnitude for the amplitude of the response near the southern boundary of model A. In preliminary experiments, we found that little is gained by specifying hypothetical variations of a and ϕ along $y = 0$. In fact, by choosing $a = 0.3$ m and with an arbitrarily chosen phase angle $\phi = 0$, we obtain results that are not noticeably inferior to other cases considered. Moreover, the computed amplitude of the M_2 elevation at Jaffna in Sri Lanka is 0.14 m compared with the observed value of 0.15 m. Accordingly, we have used this setting throughout the verification procedure but it is anticipated that a precise specification of a and ϕ along the open-sea boundary would be beneficial to the performance of the model, especially near $y = 0$.

In the combination of models A and B, the time step used in the temporal discretization is 90 s, this being consistent with the maintenance of computational stability. The computed response is effectively oscillatory after ten tidal cycles of integration. During the eleventh cycle, the response is analysed by evaluating the leading terms in the Fourier decomposition

$$\zeta = \bar{\zeta} + \sum_{k=1}^{\infty} a_k \cos\left(\frac{2\pi k t}{T} - \phi_k\right). \tag{15}$$

In (15), a_1 and ϕ_1 are the amplitude and phase of the local M_2 constituent. The time origin is arbitrary and ϕ_1 has no absolute significance. The mean tide, $\bar{\zeta}$, and further nonlinearly generated terms in (15) are of no practical value in the verification procedure.

For the purpose of validating the response in model B, we have used the Admiralty tide tables (1982) in which amplitudes and Greenwich phases of the M_2 constituent are given for selected coastal stations in the headbay. To compare these with our predictions, the computed and

observed phases have each been re-expressed relative to an arbitrarily chosen phase angle of 50° at Shortt Island.

In figure 4, we show the isolines of the computed amplitude of the M_2 constituent in the headbay. At the named coastal stations, we have also inserted observationally determined values of the M_2 amplitude. The computed amplitudes generally correlate well with the observations at stations apart from Paradeep and St Martin's Island, where the predicted amplitudes are 1.32 and 1.20 m respectively. We are unable to account for these anomalous computed values that are both in excess of the reported observational determinations. Nevertheless, with the exception of these, the discrepancies between computation and observations are generally of the order of 1%. Observational data from the complicated delta region will be strongly influenced by local orographical detail, not represented in model B. Accordingly, these have not been used in the comparison but we note that the computed amplitude of 0.77 m in the river at Ilsa Ghat compares well with the observed value of 0.78 m.

The anticipated general increase in the value of a_1 in shallow water is confirmed and amplitudes of 1.33 and 1.43 m occur at Chittagong and Hugli, respectively. The computed amplitude of 0.93 m at Dhamra (as well as the observed value of 0.90 m) implies a localized reduction in the M_2 amplitude along this part of the Orissa coast. The good agreement here is noteworthy because this is a principal region of interest in the tide–surge interaction experiment.

The isolines of the computed phase are shown in figure 5. Again, observed values are inserted at the named coastal stations and these are generally in reasonable agreement with the computed values. A sharp spatial gradient is evident in the region of the Hugli river. The phase changes by 75° over such a short distance that some doubt is cast on the ability of the model to predict accurately the phases in this region. This may explain why there is some discrepancy between the computed and observed phases at Hugli.

Although of no practical value in the verification procedure, the isolines of the computed mean tide are of general interest and help to quantify the contribution to be expected from the nonlinear processes. The isolines are plotted in figure 6, which shows that the mean tidal elevation above the equilibrium level is predicted to be as much as 0.2 m in the mouth of the river Meghna. A similar order of magnitude is predicted here for the amplitude, a_2, of the M_4 constituent.

Although we do not submit that the comparison with observation is faultless, we believe there is sufficient evidence, at least with regard to the amplitudes, to assert that the dynamical response in model B is basically correct. We therefore feel justified in using this model to analyse tide–surge interaction along the Orissa coast of India.

4. The tide in the upper Bay of Bengal on 3 June 1982

The tides in the Bay of Bengal are supported predominantly by the semidiurnal constituents M_2 and S_2 with small contributions from the diurnal constituents K_1 and O_1. Along the Orissa coast of India, the tidal elevation above equilibrium level may therefore be approximated in the form

$$\zeta = \bar{\zeta} + A\cos\{(2\pi t/T) - \beta\}. \tag{16}$$

In (16), $\bar{\zeta}$ is again the mean tide, T a semidiurnal period, β a phase function and A is a

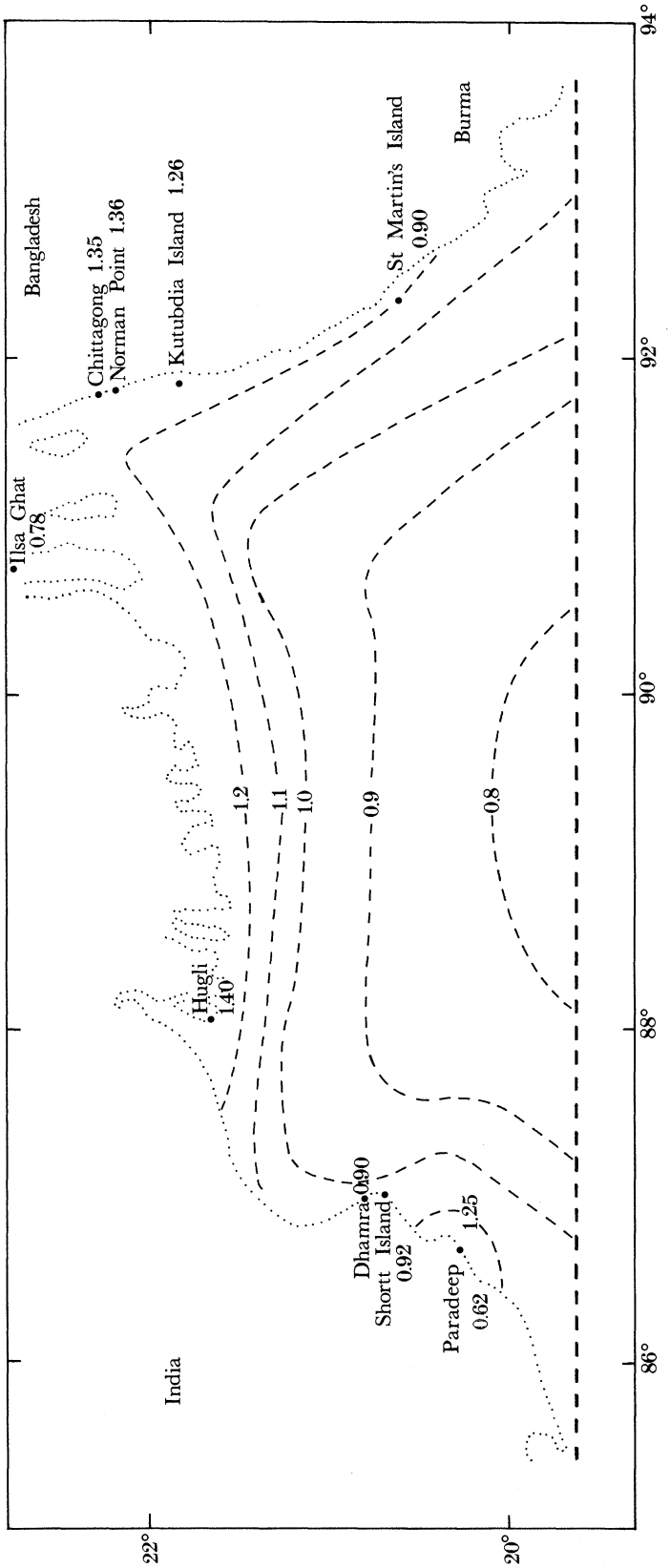

FIGURE 4. The isolines of the computed amplitude of M_2 in the headbay. The numbers on the contours refer to the amplitude in metres. The numbers inserted along the coast refer to observationally determined M_2 amplitudes in metres.

PHILOSOPHICAL TRANSACTIONS OF THE ROYAL SOCIETY A MATHEMATICAL, PHYSICAL & ENGINEERING SCIENCES

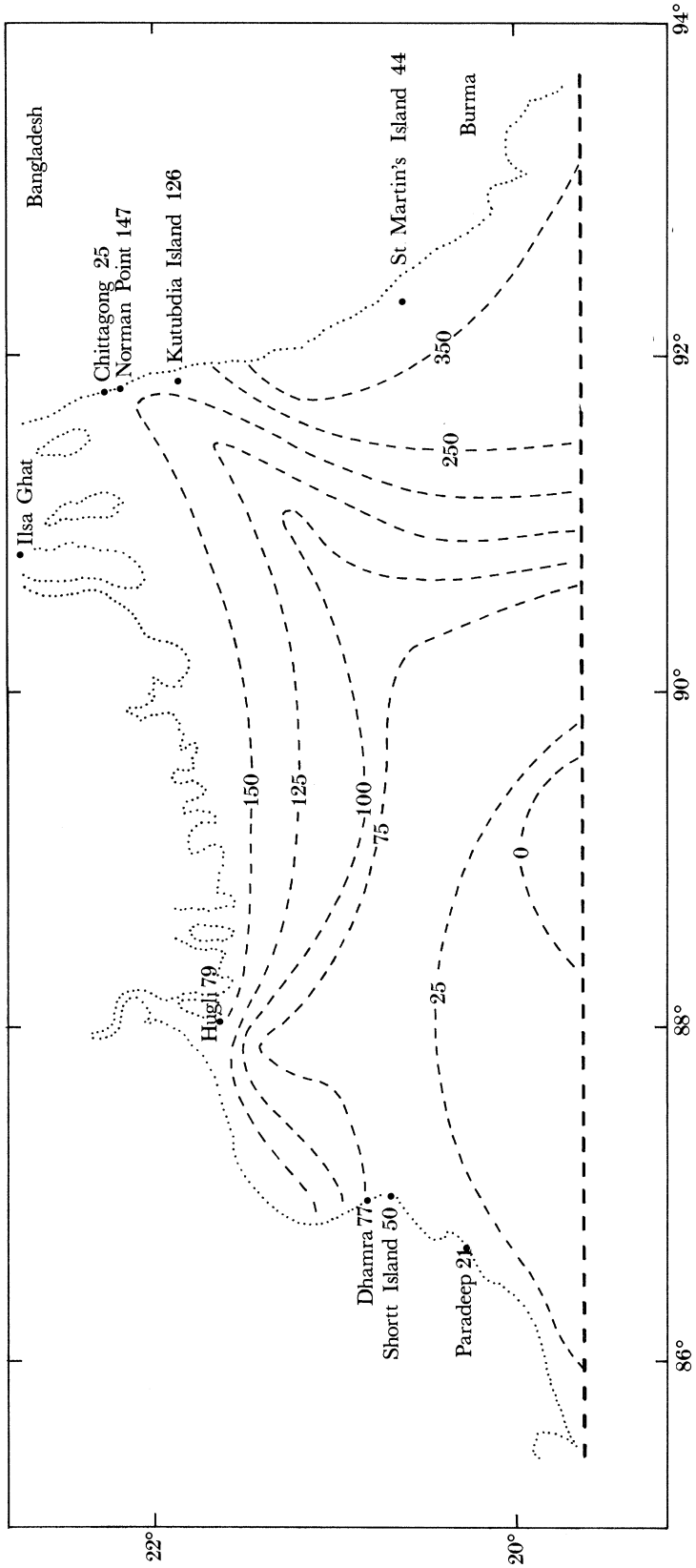

FIGURE 5. The isolines of the computed phase of M_2 in the headbay. The numbers on the contours refer to the phase in degrees. The numbers inserted along the coast refer to observationally determined M_2 phases in degrees.

PHILOSOPHICAL TRANSACTIONS OF THE ROYAL SOCIETY A MATHEMATICAL, PHYSICAL & ENGINEERING SCIENCES

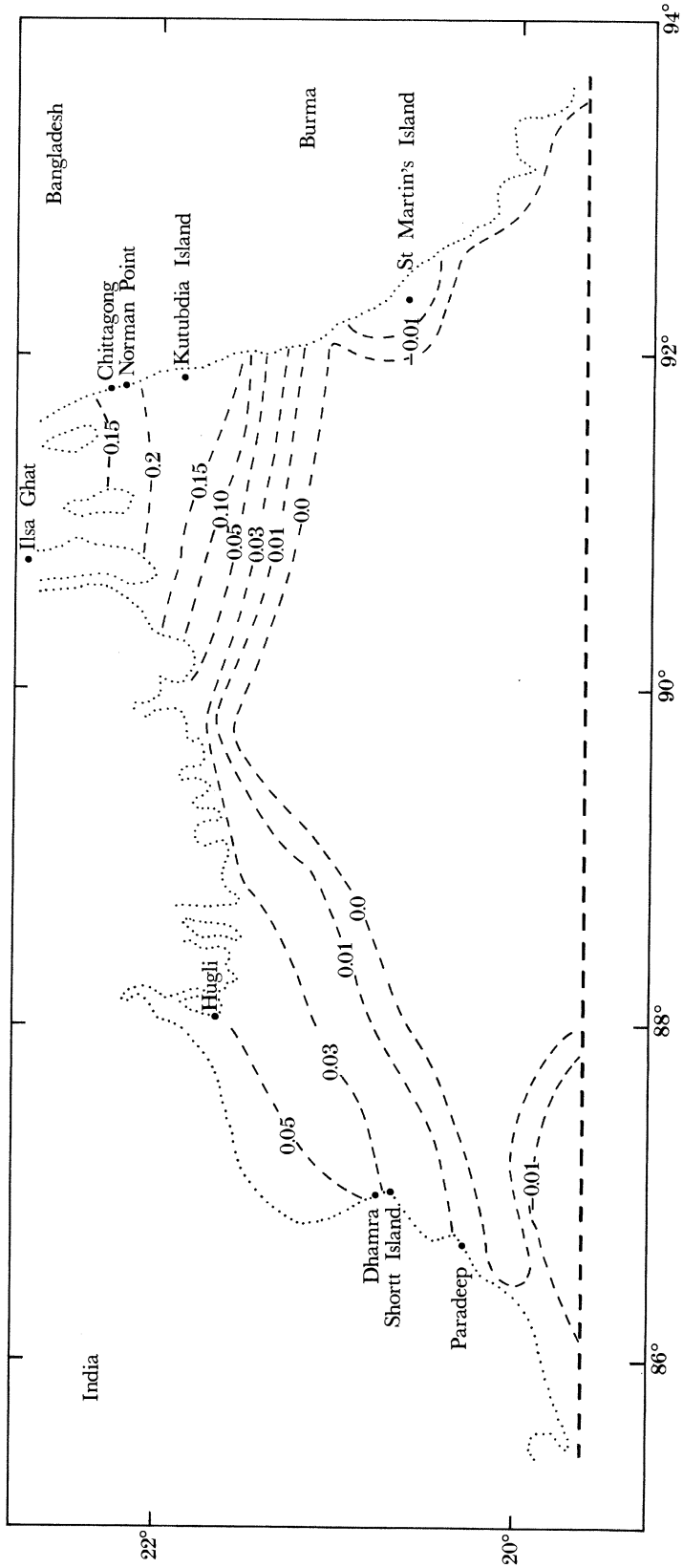

FIGURE 6. The isolines of the computed mean tide in the headbay. The numbers on the contours refer to the mean height of the elevation, in metres, above equilibrium level.

PHILOSOPHICAL TRANSACTIONS OF THE ROYAL SOCIETY A MATHEMATICAL, PHYSICAL & ENGINEERING SCIENCES

modulated amplitude that varies slowly during the spring–neap cycle because of the changing phase relation between M_2 and S_2 implied by their slightly different periods. The validity of this procedure, when used to approximate the semidiurnal tide throughout the entire Bay of Bengal, requires there to be a reasonably constant phase difference between the Greenwich phases of the local M_2 and S_2 constituents. The tide tables show this to be so, with a tabulated difference averaging about 40°.

In our applications, we propose to use models A and B to simulate the actual tide at Dhamra on 3 June 1982 when part of the Orissa coast was also affected by a surge-induced increase in the sea-surface level. By using the Admiralty tide tables for 1982, the times and heights of high and low water at Dhamra may be deduced from those given for the standard port of Sagar Roads. By using Indian Standard Time (I.s.t.), these quantities are given in table 1 for 3 June 1982.

Table 1. Times of high and low water on 3 June 1982 at Dhamra

I.s.t.		height above local datum level/m	
h.w.	l.w.	h.w.	l.w.
08h07	02h37	3.1	1.25
20h18	15h01	3.05	1.25

The average duration of each of the tidal cycles is about 12.3 h and is marginally less than the M_2 period. The average difference between high and low water is approximately 1.83 m. Therefore, on 3 June 1982, the variation of the tidal elevation at Dhamra may be approximately represented by (16) with $A \approx 0.91$ m and $T = 12.3$ h.

It will be noted that the value of A is almost exactly equal to the amplitude of the pure M_2 constituent predicted in §3 by use of model B. If this were not so, it would be necessary to adjust the amplitude of the forcing in the model until the computed response at Dhamra coincided with the actual response. However, for 3 June 1982, a sufficiently good approximation to the actual tide is obtained simply by using the solution for the pure M_2 tide with $T = 12.4$ h given in §3 although, of course, the interpretation now is that the response is due to the combined effect of M_2 and S_2. In fact, at Dhamra, the tide tables show that the amplitude of the pure M_2 constituent is 0.90 m and that of S_2 is 0.38 m. Accordingly, during the spring–neap cycle, A is bounded by 0.52 m and 1.28 m and the actual tide on 3 June 1982 corresponded to a point about mid-way between the spring and neap extremes.

5. The surge response along the Orissa coast on 3 June 1982

The Orissa coast of India was affected by a surge-induced increase in the sea-surface level on 3 June 1982. This is one of the few occasions when a reliable tide-gauge reading was made and, at the time of the maximum sea-surface elevation, the port authority at Dhamra reported an elevation of 6.7 m above their local datum level. By subtraction of the predicted tide at this time, the peak surge contribution was estimated to be 3.9 m.

As explained in §1, we propose to investigate the surge generated by pure wind-stress forcing. Any contribution resulting from the barometrically generated component of the response is excluded from the simulation under the assumption that its effect is equivalent to a simple statical correction. Accordingly, the essential data problem in representing the effect of the cyclone is one of prescribing an appropriate translating cyclonic wind field. The surface

wind-stress may then be deduced by application of the familiar type of empirical stress formulation.

The principal parameters in the representation of the wind field are those specifying its areal extent and the maximum wind speed. With the idealization that the wind speed, V, depends only on the radial distance, r, from the centre of the cyclone, an examination of the sparse data suggests that V may be represented in the form

$$V = \begin{cases} V_0 (r/R)^{\frac{3}{2}} & \text{for} \quad r \leqslant R \\ V_0 \exp\{(R-r)/\alpha\} & \text{for} \quad R < r \leqslant R_1 \\ V_0 \exp\{(R-R_1)/\alpha\} \exp\{(R_1-r)/\beta\} & \text{for} \quad r > R_1. \end{cases} \tag{17}$$

In (17), V_0 denotes the maximum wind speed and R the radius of maximum wind. α, β and R_1 are length scales determining the areal extent of the far wind field. On the basis of wind-speed data supplied by the India Meteorological Department, we have taken $V_0 = 60$ m s^{-1} and $R = 50$ km. The other parameters in (17) do not have readily accessible values. We have taken $\alpha = 200$ km, $\beta = 10$ km and $R_1 = 175$ km. This setting implies that $V \approx (0.54)\, V_0$ at $r = R_1$. For $r > R_1$, the implied wind speed falls abruptly and, at $r = 200$ km, is less than 5% of its maximum value.

For $r \leqslant R$, (17) is equivalent to the representation used by Jelesnianski (1965). The differences for $r > R$ arise because of an apparently lower wind speed in the far field of the Orissa cyclone compared with that implied by Jelesnianski's representation. For $r > R$, Jelesnianski used $V = V_0 (R/r)^{\frac{1}{2}}$ that, for $r = R_1$, yields $V = (0.53)\, V_0$. For $r = 200$ km, however, it implies $V = 30$ m s^{-1} compared with our reduced value of less than 3 m s^{-1}. Our experience is that the representation of the far wind-field is crucial. Wind speeds that are too great lead to a high surge response along an unrealistically long section of the coast. Thus, given the fairly reliable estimates for V_0 and R, the only option available is to reduce the wind speed in the far field below that used by Jelesnianski. This reduces the length of the coast along which there is a significant surge response and, at the same time, has little effect on the magnitude of the predicted peak value.

Equation (17) determines the wind speed and implies nothing about its direction. A feature of the surface wind-field distribution in a tropical cyclone is the variability in the radial component of the flow. For $r < R$, this is negligible but for $R < r < 3R$, there is a generally increasing component of the inward directed radial velocity. For $r > 3R$, the angle of inflow is fairly constant and equal to about 30°. To appraise the effect of this on the surge generating capacity of the cyclone, we have prescribed an inflow angle, δ, so that the radial and transverse components of the surface wind stress are determined from

$$\left.\begin{aligned} \tau_r &= -c_{\mathrm{D}}\, \rho_{\mathrm{a}}\, V^2 \sin\delta \\ \tau_\theta &= c_{\mathrm{D}}\, \rho_{\mathrm{a}}\, V^2 \cos\delta \end{aligned}\right\}. \tag{18}$$

In (18), the drag coefficient, c_{D}, is assumed uniform and equal to 0.0028 and ρ_{a} is the density of air at 1000 mbar.

The circulatory system is moved across the analysis area along a track approximating that followed by the actual storm. This is shown in figure 2 where the starting point corresponds to the position of the storm's centre at 10h30 I.s.t. on 3 June 1982. In the model simulation, this time corresponds to $t = 0$ when the state of the system is prescribed as being one of rest.

It will be noticed that the initial position of the cyclone's centre is not within the area covered by model B. However, its surge-generating capacity is recorded from the outset in model A. The time of landfall is about 21h30 on 3 June and so the model surge response evolves for about 11 h before that event. An extended period of model evolution is found to have little effect on the predicted surge at Dhamra near the time of landfall. The position of landfall is approximately 17 km along the coast to the northeast of Paradeep.

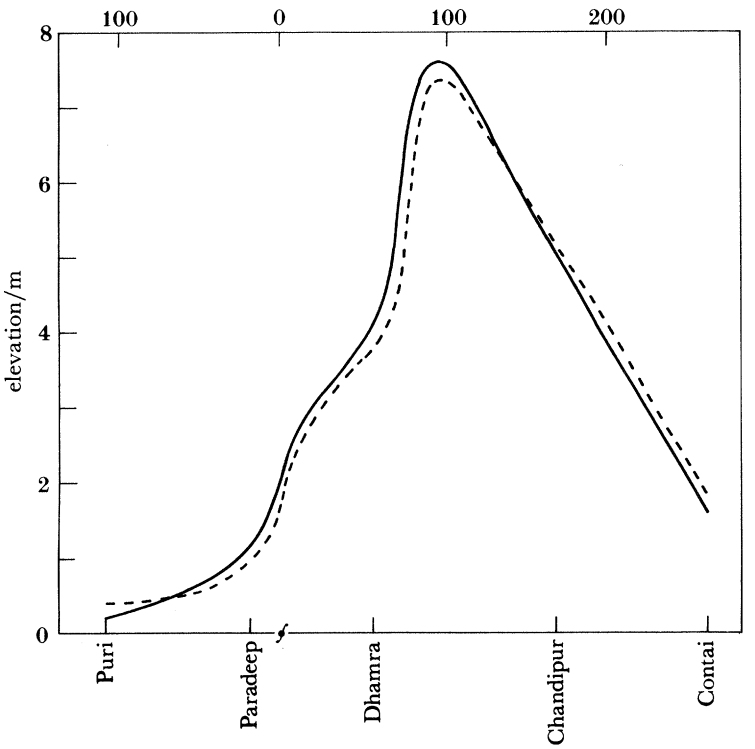

FIGURE 7. The computed peak surge envelope along the Orissa coast; ——, maximum value of ζ_s, $\delta = 15°$; -----, maximum value of ζ_s, $\delta = 0°$; ϕ denotes the position of landfall.

We have performed preliminary experiments to determine the effect of an inflow angle on the pure surge response, ζ_s, by taking $\delta = 0$ and 15°. The results of these are presented in figure 7 in the form of the computed peak surge response along the Orissa coast. Inspection of this shows that the inflow angle is relatively unimportant. The peak surge response is about 7.5 m and occurs about 100 km to the right of the position of landfall. The peak elevation at Dhamra is about 3.8 m with $\delta = 0$ and 4.1 m with $\delta = 15°$. Although an incorporation of the inflow angle increases the surge response, uncertainties in the values of the other parameters suggest that little is gained by arbitrarily assigning a non-zero value to δ and we hereafter take $\delta = 0$. The sea-surface response to the left of the landfall is, in accordance with expectations, relatively small and the significant response extends about 200 km along the coast to the right of the landfall position.

Given that the effect of barometric forcing has been omitted in the simulation, the computed values are possibly rather high compared with the surge residual of 3.9 m at Dhamra reported when the sea-surface level was greatest. The influence of tide–surge interaction on these values must therefore be determined.

6. Tide–surge interaction along the Orissa coast on 3 June 1982

In this section, we propose to combine the simulations described in §§4 and 5 to determine the nature of the interaction existing between the tide and surge during the period of abnormally high sea-surface levels encountered along the Orissa coast on 3 June 1982.

Essentially, the exercise consists of a determination of the consequences of using the tidal solution given in §3 to provide the initial sea-state conditions for the surge calculation described in §5. The only procedural requirement is that of adjusting the phase of the tidal solution computed in §3 so that the initially prescribed dynamical state corresponds to the actual tidal conditions at the model time $t = 0$. From table 1, the second of the high tides at Dhamra on 3 June occurred at 20h18 I.s.t. This is 9.8 h after the time of commencement of the wind-stress forcing in the proposed model simulation. Accordingly, when $t = 9.8$ h in the model, it must be high tide at Dhamra. The correct phase in the tidal solution derived in §3 to produce this condition may be arranged by specifying an appropriate non-zero value for ϕ in (7), rather than zero as in §3. The semidiurnal component of the tidal response in the model is then given by

$$\zeta = a_1 \cos\{(2\pi t/T) + \phi - \phi_1\}. \tag{19}$$

The value of ϕ_1 computed in §3 at Dhamra is -1.01 rad. High tide at Dhamra must occur at $t = 9.8$ h and (19) immediately leads to a value of $\phi = 0.307$ rad. This value of ϕ is used subsequently in the forcing of the tidal component of the solution during the tide–surge interaction experiments. The purely tidal component of the solution is referred to as ζ_t. The dynamical state of the system at the time of commencement of the wind-stress forcing is simply found by evaluating the pure tidal response at $t = 0$. The prescribed wind-stress forcing is identical to that used in §5.

The results of the simulations may be presented in several different ways, each illustrating a different aspect of the tide–surge interaction. From the point of view of the potential flooding risk, the crucially important parameter is the maximum total elevation of the sea surface predicted at points along the coastline. The elevation will be partly of tidal origin and partly of surge origin, the two combining in an essentially nonlinear way, and is referred to as $\zeta_{s+t+I.s.t.}$. The envelope of the maximum elevation is shown in figure 8 from which it is seen that the predicted peak elevation above equilibrium level at Dhamra is approximately 4.33 m and that at Paradeep is 1.95 m. The computed pure tidal elevations (that include a small nonlinear contribution generated in shallow water) at these stations at the times of occurrence of the peak total elevations are, respectively, 0.97 and 1.21 m. These results imply corresponding surge residuals of 3.36 and 0.74 m. Data acquired from a tidal staff at Dhamra and a tide gauge at Paradeep near the times of the peak recorded elevations imply surge residuals of 3.9 and 1.0 m. Given that we have omitted the effect of barometric forcing from our calculations that, on the basis of a statical correction, would add a further 0.5 m for a local 50 mbar drop in atmospheric pressure, the comparison appears reasonably satisfactory.

Additionally, we show in figure 8 the computed times at which the peak elevations are attained at different stations along the coast. The observational estimates at Dhamra and Paradeep are also indicated in figure 8 and these are seen to agree well with the corresponding computed times. An inference to be drawn here is that the maximum surge response appears to progress along the Orissa coast. On moving northeast from Paradeep, the time of occurrence

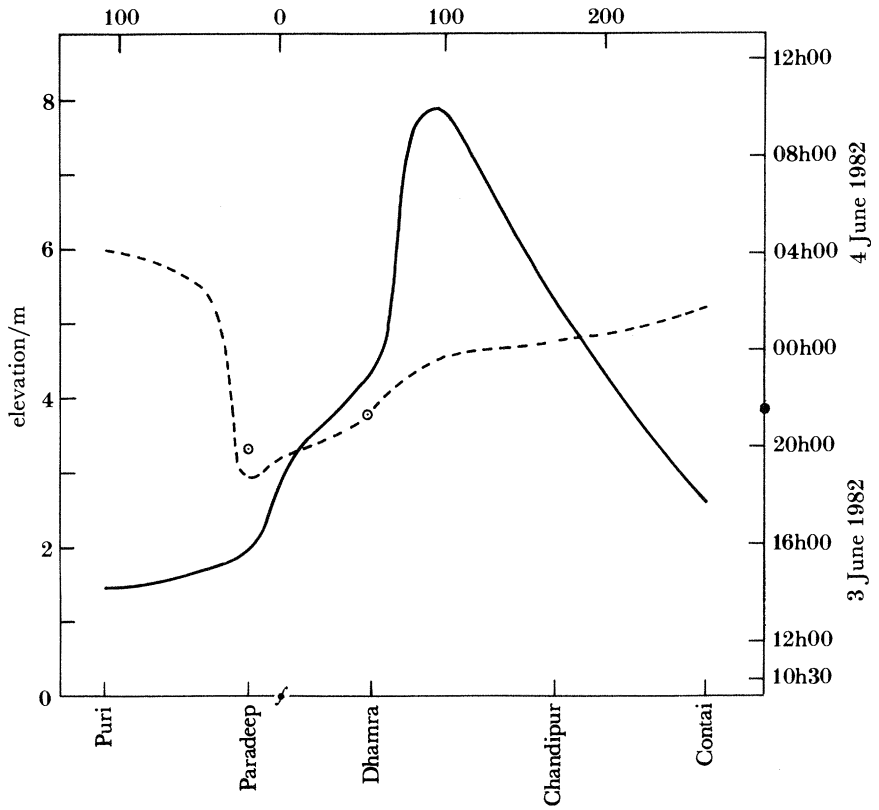

FIGURE 8. The computed envelope of the maximum elevation along the Orissa coast and the computed times of occurrence; ——, maximum value of $\zeta_{s+t+I.s.t.}$; -----, times of occurrence of maximum values; ϟ denotes the position of landfall; ● denotes the time of landfall.

of the peak elevation becomes progressively later, suggesting that the response has the form of a solitary elevation wave propagating along the coast.

As an alternative to considering the envelope of the peak surface elevation, it is also useful to evaluate the surface elevation at points along the coast at the time of occurrence of the maximum elevation at Dhamra, which is predicted to be at 21h20 I.s.t. This quantity is shown in figure 9 together with the purely tidal contribution. The corresponding surge residual is also plotted and, as before, is determined by subtracting the purely tidal contribution from the response due to the simultaneous presence of both tide and surge as given by $\zeta_{s+I.s.t.} = \zeta_{s+t+I.s.t.} - \zeta_t$. As already noted, the maximum surface elevation above equilibrium level at Dhamra is 4.33 m and, at this time, the maximum elevation occurring further along the coast is 6.24 m. This should be compared with our previously predicted total elevation of 7.9 m at this same position, which is attained at about 23h30. Again, this result clearly suggests the northeasterly progression of the surge response along the coast.

Principal attention has so far been focused on the predicted surge response at Dhamra because of the tide-gauge reading that is available for this station. However, as mentioned before, the predicted maximum sea-surface elevation occurs about 50 km along the coast from Dhamra. It is therefore informative to determine the elevation along the coast at the time at which this maximum value is attained. The model calculation shows that the absolute maximum elevation

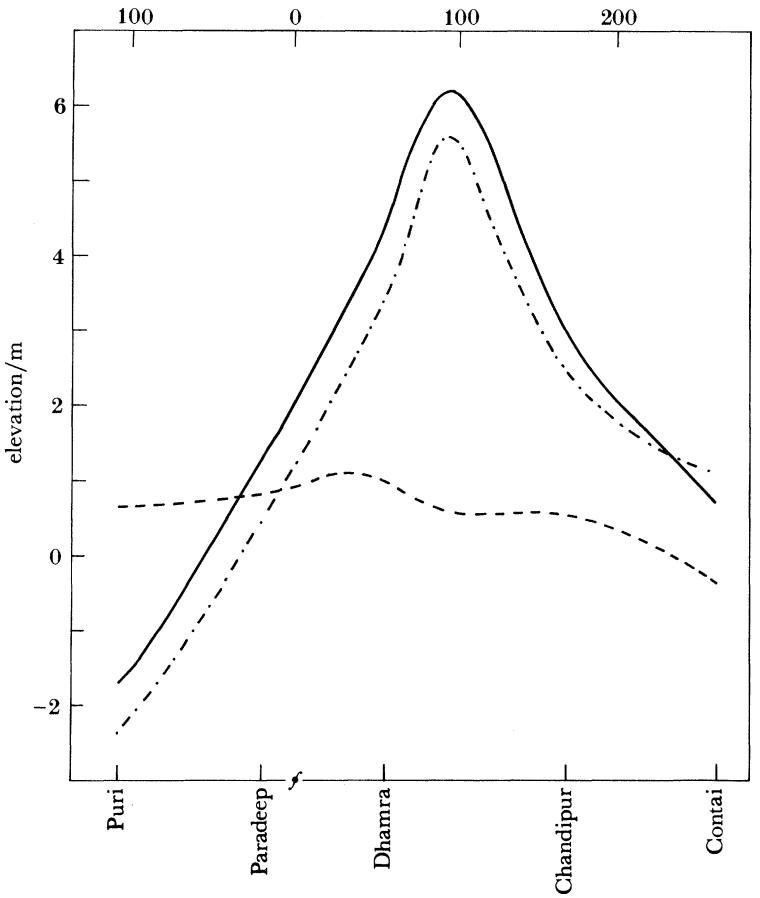

FIGURE 9. The computed elevation along the Orissa coast at the time of occurrence of the maximum elevation at Dhamra; ——, $\zeta_{s+t+I.s.t.}$; - - - -, ζ_t; —·—, $\zeta_{s+I.s.t.}$; ↓ denotes the position of landfall.

is attained at 23h30 on 3 June, which is 2.17 h after the occurrence of the local maximum at Dhamra and 2 h after landfall of the cyclone. A plot of the sea-surface elevation along the Orissa coast at this time is given in figure 10. Also shown is the component due to the pure tide, ζ_t, and the implied surge residual $\zeta_{s+I.s.t.}$. Thus, an absolute peak surge residual of approximately 7.76 m is predicted to occur about 95 km to the right of the landfall position. At the time of its occurrence, a surge residual of more than 1 m is predicted to affect a 240 km length of the coast.

Unfortunately, we are unable to support these results by quantitative observational evidence and recognize that the prediction of a maximum surge residual of 7.76 m may be contentious. On the other hand, there is no other plausible choice of parameters in (17) that leads to a correctly predicted surge residual at Dhamra without a similar attendant result.

The dynamical consequences of the tide–surge interaction process are not effectively illustrated in a plot showing the spatial variation of the sea-surface elevation $\zeta_{s+t+I.s.t.}$ at a fixed time. Accordingly, we now consider the temporal variation of $\zeta_{s+t+I.s.t.}$ at a fixed position. This quantity is shown in figure 11 for Dhamra during the period 3–4 June 1982. Also shown is the temporal variation of ζ_t as well as that of the linear superposition of the pure surge and the pure tide defined by $\zeta_{s+t} = \zeta_s + \zeta_t$. Incorporation of the interactive effect is seen to advance

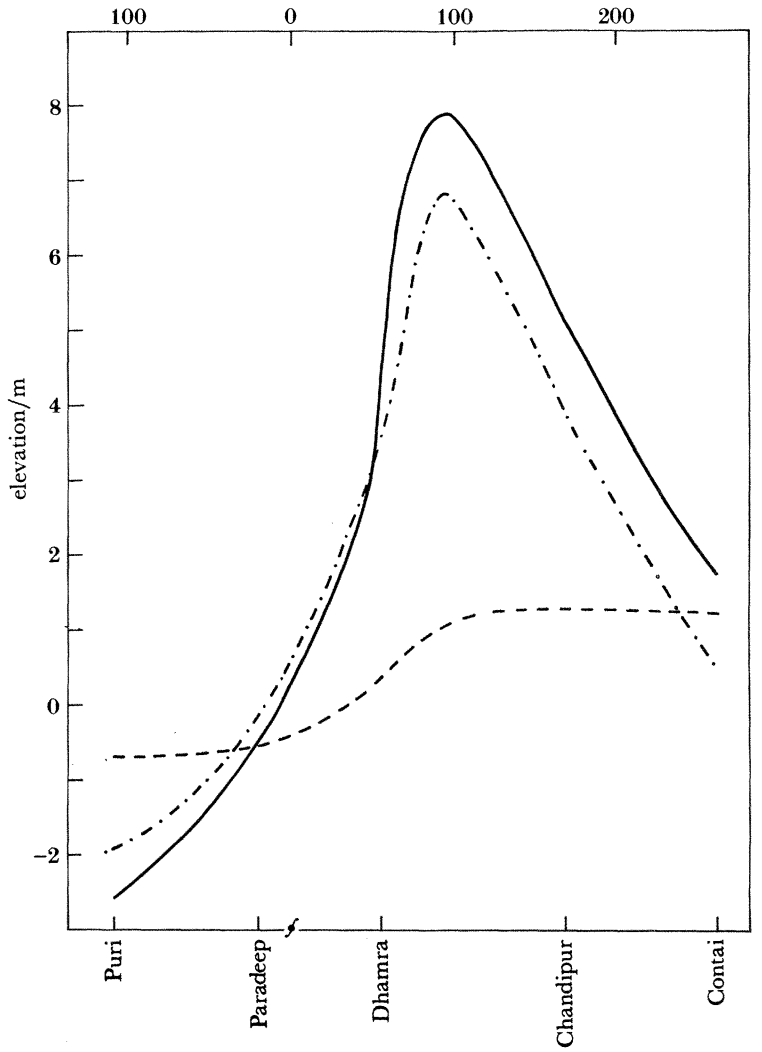

FIGURE 10. The computed elevation along the Orissa coast at the time of occurrence of the absolute peak elevation; ——, $\zeta_{s+t+I.s.t.}$; - - - -, ζ_t; —·—, $\zeta_{s+I.s.t.}$; ∮ denotes the position of landfall.

the time of occurrence of the peak total elevation to 21h20 compared with about 20h30 when based on an evaluation of ζ_{s+t}. This difference of 50 min brings the predicted time of occurrence of the peak elevation into closer accord with the observational estimate of 22h00. A further consequence of the interaction is a reduction in the peak value of $\zeta_{s+t+I.s.t.}$ to 4.33 m compared with a corresponding evaluation of ζ_{s+t} that yields about 4.51 m. Near the time of the maximum response, it will be noted that the interaction leads to a reduction in the total elevation on the rising tide and an increase on the falling tide. General results of this kind have been noted previously by Banks (1974) and Johns & Ali (1980).

The temporal variation of the sea-surface elevation, $\zeta_{s+t+I.s.t.}$ at the position of peak response is shown in figure 12 together with a plot of ζ_t and ζ_{s+t}. On comparison with figure 11, the progression of the surge wave along the coast is again evident. The general effect of the interaction is similar to that at Dhamra. On the rising tide, $\zeta_{s+t} > \zeta_{s+t+I.s.t.}$ and on the falling

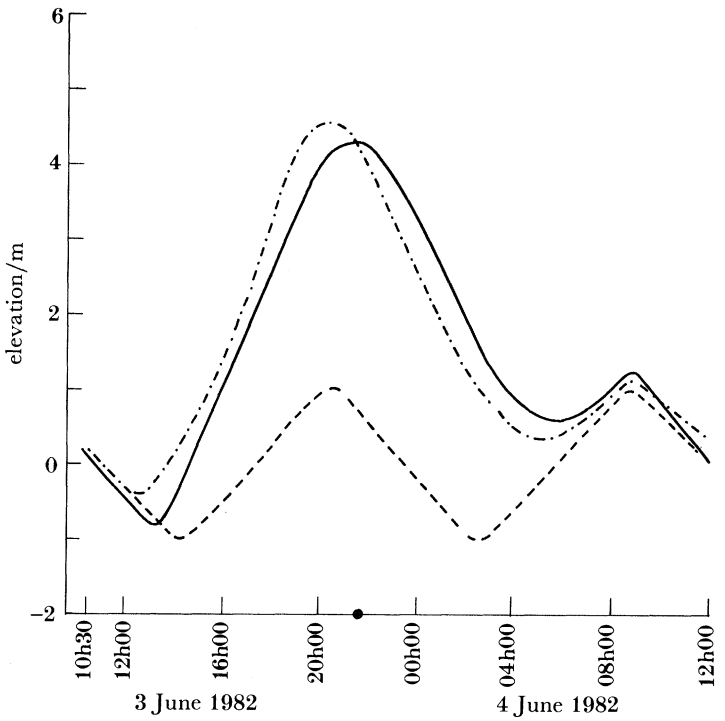

FIGURE 11. The computed variation of the elevation with time at Dhamra; ——, $\zeta_{s+t+I.s.t.}$; - - - - -, ζ_t; —·—, ζ_{s+t}; ● denotes the time of landfall.

tide $\zeta_{s+t} < \zeta_{s+t+I.s.t.}$. In contrast with the corresponding result at Dhamra, however, the interactive effect does not lead to any change in the time of occurrence of the peak elevation compared with a determination based on the value of ζ_{s+t}.

Finally, it is of interest to examine the combined tide and surge response at the port of Contai, which is located in the most westerly of the rivers (the Hugli) included in the headbay model. In figure 13, the temporal variation of $\zeta_{s+t+I.s.t.}$ is plotted together with that of ζ_t and ζ_{s+t}. It should be noted that the maximum surge response is predicted to occur at about 02h40 on 4 June. This is approximately 5.3 h after the maximum response at Dhamra. The separation distance between the two stations is about 220 km and so the implied speed of progression of the elevation wave is approximately 11.5 m s^{-1}. A simple, theoretically based, estimate may be made for the phase speed if it be assumed that the response progresses along the coast in the form of a freely propagating shallow water gravity wave. The phase speed is then given approximately by the value of $(g\bar{h})^{\frac{1}{2}}$ where $\bar{h}$ is an appropriate mean depth in the coastal zone. Northeast of Paradeep, the bathymetry shown in figure 1 implies that $\bar{h}$ lies between about 10 and 20 m. Accordingly, the phase speed is bounded by about 10 and 14 m s^{-1}. It is interesting to note that the speed deduced from the numerical model also lies between these values thus providing further evidence for our submission concerning the dynamical character of the response after landfall of the cyclone.

At Contai, the relatively shallow water has the effect of both increasing the amplitude of the semidiurnal tide and strengthening the contribution of nonlinearity. There is evidently a significant nonlinearly generated mean tidal elevation, $\bar{\zeta}$, of about 0.5 m. Although the surge-induced component is now much reduced compared with that at Dhamra, the interaction

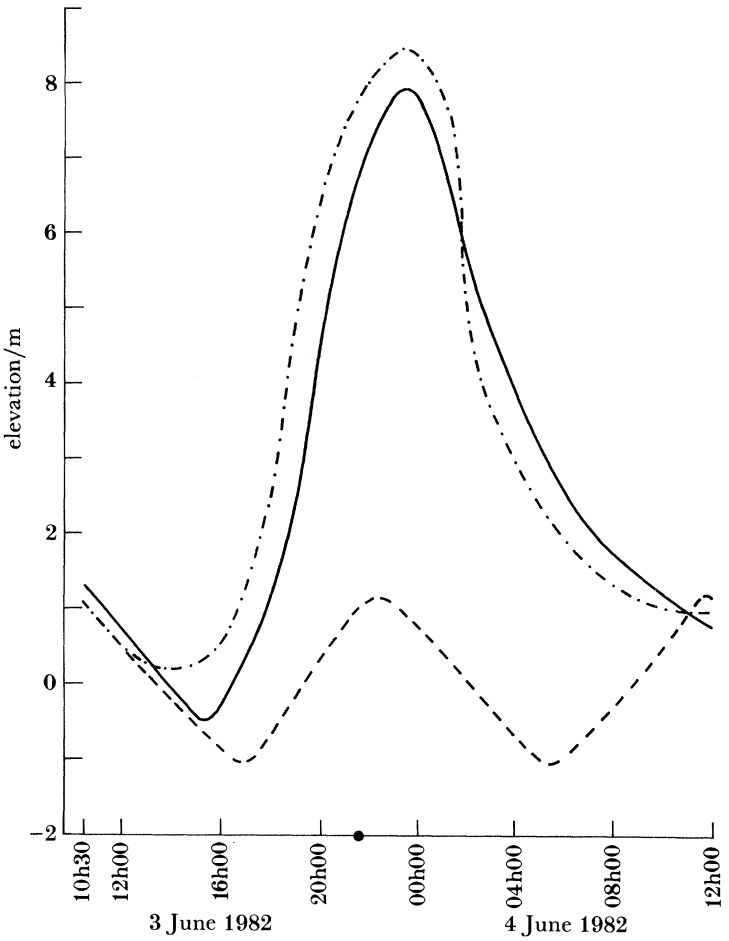

FIGURE 12. The computed variation of the elevation with time at the position of peak response; ——, $\zeta_{s+t+I.s.t.}$; -----, ζ_t; —·—, ζ_{s+t}; ● denotes the time of landfall.

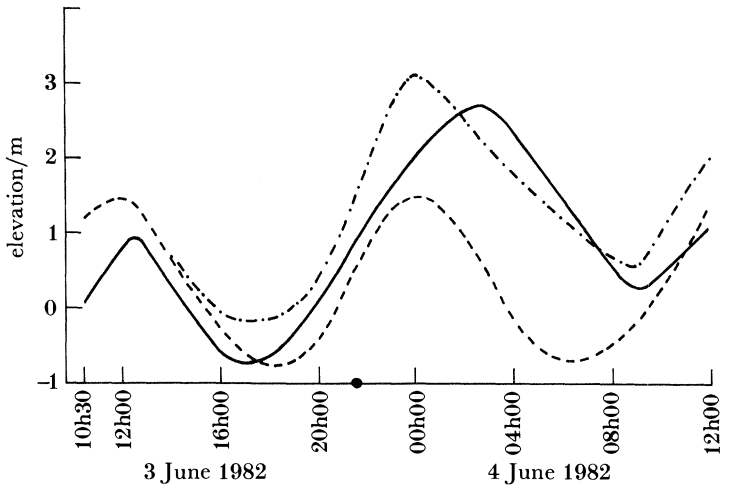

FIGURE 13. The computed variation of the elevation with time at Contai; ——, $\zeta_{s+t+I.s.t.}$; -----, ζ_t; —·—, ζ_{s+t}; ● denotes the time of landfall.

between tide and surge is at its strongest. The maximum elevation occurs about 2.7 h after the time suggested by an evaluation of ζ_{s+t}. The value of the maximum elevation is almost 0.45 m below the value derived from ζ_{s+t}. This difference is about 21 % of the predicted elevation above the mean tidal level. This is clearly a significant difference and must be incorporated into any effective predictive scheme.

7. The surge response along the Andhra coast between 18–20 November 1977

Part of the Andhra coast in the neighbourhood of Divi Island was affected by surge-induced flooding on 19 November 1977. Tide-gauge readings of peak sea-surface levels are not available but, on the basis of inland watermarks and debris found entangled in trees, the sea-surface at this time was estimated to have been in excess of 5 m above its mean level.

An earlier attempted simulation of this surge event has been described by Johns *et al.* (1981) on the basis of the pure wind-stress forcing resulting from a model cyclone approximating that which struck the coast of Andhra Pradesh on 19 November. The numerical models in the simulation had a relatively coarse north–south resolution and utilized the curvilinear boundary treatment applied in model A. Some deficiencies in the predictions were apparent. In particular, the models predicted that the maximum surge elevation occurs to the left of the landfall position. This appears to be contrary to eyewitness accounts of the coastal inundation. In this section, we propose to reconsider the simulation of the Andhra surge by using a combination of models A and C.

As in the case of the Orissa surge simulation, we consider first the response due to pure wind-stress forcing. A similar representation of the surface wind-speed is used to that in §5. For this,

$$V = \begin{cases} V_0(r/R)^{\frac{3}{2}} & \text{for} \quad r \leqslant R \\ V_0 \exp\{(R-r)/\alpha\} & \text{for} \quad r > R. \end{cases} \tag{20}$$

Following work reported by Johns *et al.* (1982), we take $V_0 = 70$ m s^{-1}, $R = 80$ km and $\alpha = 240$ km. Thus, at $r = 400$ km, the wind speed is reduced to about 18 m s^{-1}, which is reasonably compatible with the composite data set presented by Johns *et al.* (1981). It also avoids the unrealistically high surge response far along the coast from Divi that would result if, following Jelesnianski (1965), $V = V_0(R/r)^{\frac{3}{2}}$ for $r > R$. The inflow angle is taken as zero and the associated surface wind stress is determined by (18) with $\delta = 0$.

The idealized track followed by the centre of the cyclone starts in model A and its final section is shown in figure 3. The wind-stress forcing is recorded from 16h30 I.s.t. on 16 November 1977 and continues until landfall at 15h00 I.s.t. on 19 November. The time step used in the integration is 60 s.

In figure 14, we show the computed envelope of the peak surge response along the Andhra coast together with the times at which the maximum values are attained. A maximum elevation of about 5.3 m is predicted at Divi while that at Kavali is 2.53 m. These values should be contrasted with maximum elevations of 4.8 and 5.3 m at Divi and Kavali respectively as predicted by Johns *et al.* (1981).

In this simulation, the lower value at Kavali is found to be a consequence of the more detailed representation of the coastal orography in model C compared with that in model A. The

qualitative nature of the new prediction is also encouraging because of the general tendency for the maximum surge response to occur to the right of the landfall position. Moreover, it is compatible with the absence of any reports of flooding along that part of the coast to the south of the landfall position. It should be noted, however, that the maximum surge is predicted to be 6.46 m and that this occurs to the northeast of Divi. As mentioned previously, tide-gauge readings are not available to substantiate this result and such a response would only have been apparent in actuality if this part of the coast were susceptible to flooding.

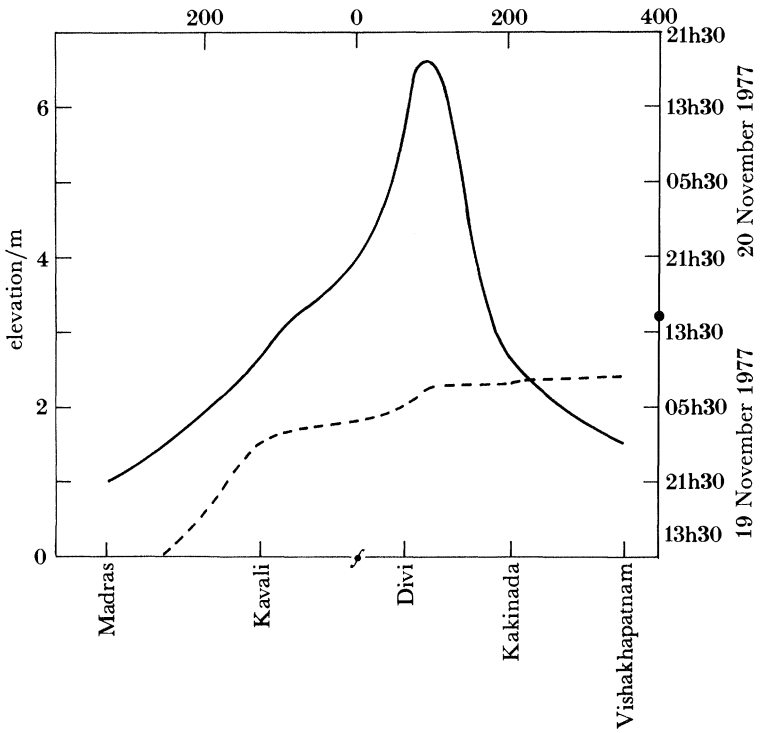

FIGURE 14. The computed peak surge envelope along the Andhra coast and the computed times of occurrence of the peak values; ——, maximum value of ζ_s; -----, times of occurrence of maximum values; ϕ denotes the position of landfall; ● denotes the time of landfall.

We also see that the peak surge elevations at Madras and Vishakhapatnam are relatively small and equal to 0.67 and 1.19 m respectively. Accordingly, in comparison with the work reported by Johns *et al.* (1981), there is a confinement of the peak surge response to a much shorter length of the coast.

By examining the times of occurrence of the maximum surge response given in figure 14, it is suggested that the peak surge elevation moves northeast along the Andhra coast in the form of a solitary elevation wave. The time required for this to travel from the point of landfall to Vishakhapatnam is about 4.8 h. The separation distance between these stations is about 350 km and so the implied speed of progression is approximately 20 m s^{-1}. It is not so straightforward as for the Orissa coast to estimate an appropriate mean depth ($\bar{h}$) off Andhra but, from figure 1, a value of 50 m appears reasonable. The theoretically determined phase speed for a shallow water gravity wave is then about 22 m s^{-1}. This is close to the speed deduced from the numerical model but it is recognized that the value chosen for $\bar{h}$ is not unique. Nevertheless, we believe that it provides further evidence to support our submission that the

surge response progresses along the coast in the form of a freely propagating shallow water gravity wave.

8. Tide–surge interaction along the Andhra coast

The astronomical tide along the Andhra coast of India has a much reduced amplitude compared with that in the headbay. At Madras, the tide tables show that the amplitudes of the predominant M_2 and S_2 constituents are respectively 0.33 and 0.14 m. The tidal solution described in §3 may be evaluated in model C, although the detail in this will be less reliable than that in model B because of the greater proximity of the open-sea boundary at $y = 0$. Nevertheless, the isolines of the computed amplitude of M_2 shown in figure 15 are reasonably consistent with the few observational determinations along the Andhra coast.

In view of the smaller tidal amplitude, tide–surge interaction along the Andhra coast is likely to be weaker than that in the headbay. Although the actual tidal data in the neighbourhood of Divi Island are not available to us for the period of the 1977 surge event, it appears worthwhile to perform a numerical experiment with semidiurnal forcing to quantify the likely effect of the tide–surge interaction mechanism in this region. This has been done by using the

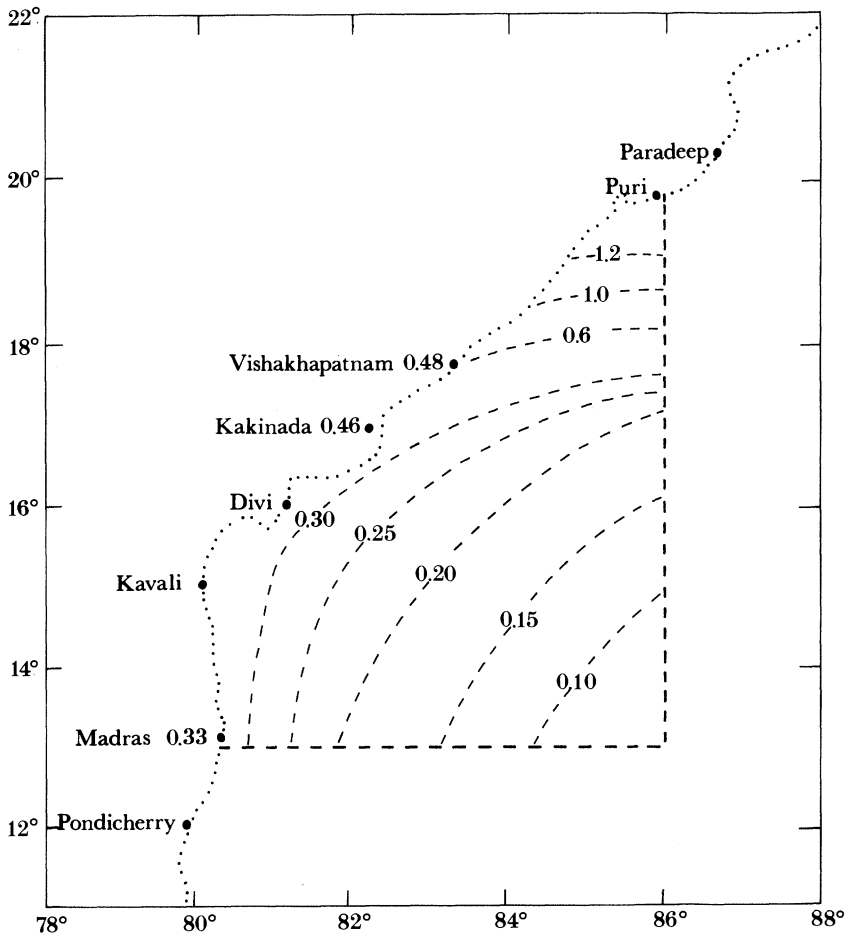

Figure 15. The isolines of the computed amplitude of M_2 in model C. The numbers on the contours refer to the amplitude in metres. The numbers inserted along the coast refer to observationally determined amplitudes in metres.

tidal solution given in §3 as the initial sea-state data for the pure surge experiment described in §7. The combined response is determined by maintaining the tidal component of the solution through use of (7) during the application of the wind-stress forcing. As an illustrative case, we take $\phi = \frac{3}{4}\pi$ in (7) because experimentation shows that this leads to a maximal interactive effect at the time and place of the peak response on the Andhra coast.

The maximum response occurs about 90 km to the northeast of the landfall position and then $\zeta_{s+t+I.s.t.} = 6.63$ m. At the same position and time, the calculation in §7 shows that $\zeta_s = 6.46$ m while $\zeta_t = -0.15$ m, implying that $\zeta_{s+I.s.t.} = 6.78$ m. The interaction therefore leads to an increased surge residual compared with the pure surge value. An increase is certainly to be expected because, generally, at low tide, $\zeta_{s+t+I.s.t.} > \zeta_{s+t}$. Nevertheless, the difference in the predicted surge residual of 0.32 m is, in absolute terms, greater than expected. Comparatively, however, it is only about 5% of the total elevation and is therefore scarcely important.

To conclude this section, we show in figure 16 the variation of $\zeta_{s+t+I.s.t.}$ along the Andhra coast at the time of occurrence of its maximum value 90 km to the northeast of the landfall position. Also illustrated is the spatial variation of both $\zeta_{s+I.s.t.}$ and ζ_t at this time. Significant

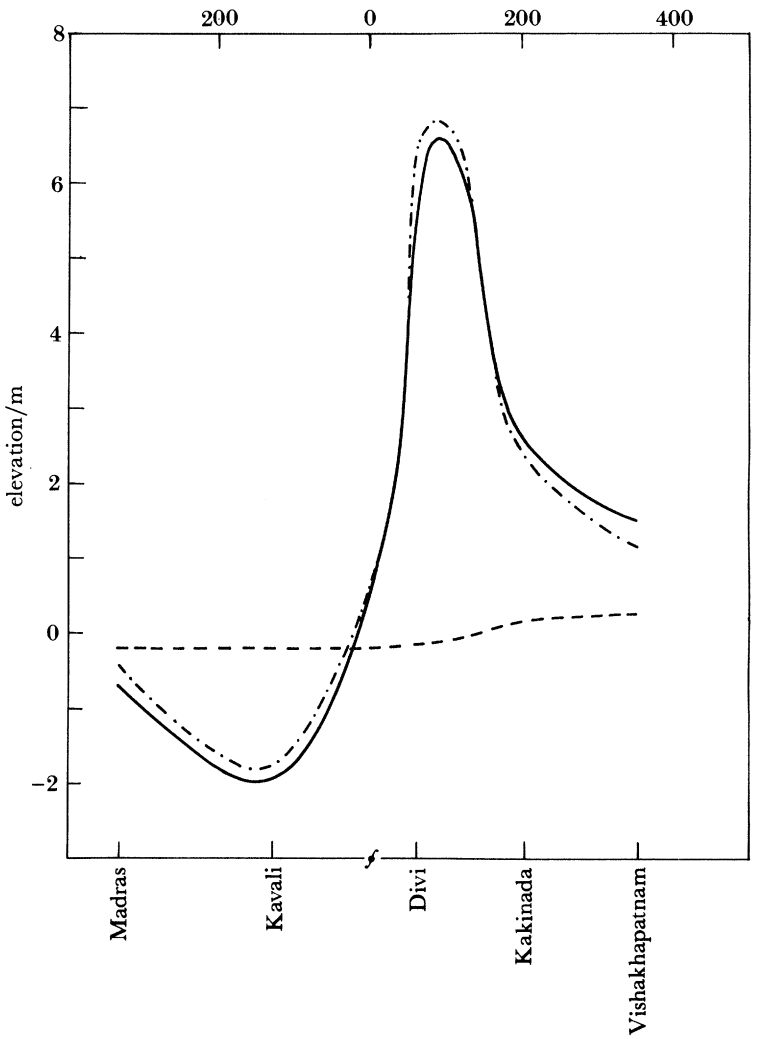

FIGURE 16. The computed elevation along the Andhra coast at the time of occurrence of the absolute peak elevation; ——, $\zeta_{s+t+I.s.t.}$; - - - -, ζ_t; —·—, $\zeta_{s+I.s.t.}$; ∮ denotes the position of landfall.

surge residuals are confined to that part of the coast to the right of the landfall position and these exceed 1 m over a distance of about 350 km. The residual at Divi is about 4 m, which is approximately 1.3 m less than that occurring earlier at this station. Therefore, in this case, when the tidal contribution is minimal, there is clear evidence of the northeasterly progression of the surge wave along the coast.

9. Concluding remarks

An application has been made of numerical models in a study of tide–surge interaction along the Orissa coast of India. A comparison is made of the model predictions with the limited tide-gauge data available for the severe surge of June 1982. The agreement between these is encouraging and experiments are performed that throw light on the dynamical character of the evolving response. The interaction between tide and surge is found to lead to a substantial effect off the Orissa coast. This becomes even greater in the complex river system in the headbay and, at Contai, should be taken into account in any predictive scheme.

A similar study has been carried out for the Andhra surge of November 1977. Tide–surge interaction here is much weaker and an effective predictive scheme can be based on the calculation of the pure surge response.

During these studies it has become clear that further progress in the modelling of pure surges and tide–surge interaction in the Bay of Bengal is dependent upon a relevant data acquisition programme. Tidal data for the model generation of the astronomical tides in the Bay are, at present, inadequate. The essential information required relates to both elevation and current data along the southernmost boundary of the Bay where it communicates with the northern Indian Ocean.

A further area of data inadequacy is in the prescription of the surface wind-stress. Any improvement in the representation of this depends upon the availability of extended data sets for surface conditions in Bay of Bengal cyclones. Reliable estimates of wind speeds and directions are required together with an accurate determination of the radius of maximum wind. Additionally, an improved knowledge of the far wind-field is necessary because this, acting over an extensive area of water, contributes importantly to the surge generation. Although of secondary importance, the corresponding surface atmospheric pressure in the cyclone is also required. Availability of this would facilitate the inclusion of the dynamics of the barometrically forced component of the surge as an alternative to relying on the application of a purely statical correction.

Finally, there remains the need for a more complete validation of the surge predictions. This requires the monitoring of an actual surge event by a network of strategically deployed coastal tide gauges. The surge responses computed in this paper have only been compared with a few peak sea-surface elevations. There is a need for continuous tide-gauge recordings throughout the duration of the event. Additionally, these recordings are required at a sequence of coastal stations along that part of the coast affected by the surge. Only then will there be sufficient relevant data to effect a complete validation of the surge prediction schemes described in this paper.

A large part of this work was done with support provided by the U.K. Overseas Development Administration.

PHILOSOPHICAL TRANSACTIONS OF THE ROYAL SOCIETY A MATHEMATICAL, PHYSICAL & ENGINEERING SCIENCES

References

Banks, J. E. 1974 A mathematical model of a river-shallow sea system used to investigate tide, surge and their interaction in the Thames–southern North Sea region. *Phil. Trans. R. Soc. Lond.* A **275**, 567–609.

Das, P. K., Sinha, M. C. & Balasubramanyam, V. 1974 Storm surges in the Bay of Bengal. *Q. Jl R. met. Soc.* **100**, 437–449.

Flierl, G. R. & Robinson, A. R. 1972 Deadly surges in the Bay of Bengal: dynamics and storm-tide tables. *Nature, Lond.* **239**, 213–215.

Heaps, N. S. 1969 A two-dimensional numerical sea model. *Phil. Trans. R. Soc. Lond.* A **265**, 93–137.

Jelesnianski, C. P. 1965 A numerical calculation of storm tides induced by a tropical storm impinging on a continental shelf. *Mon. Weath. Rev. U.S. Dep. Agric.* **93**, 343–358.

Jelesnianski, C. P. 1966 Numerical computations of storm surges without bottom stress. *Mon. Weath. Rev. U.S. Dep. Agric.* **94**, 379–394.

Jelesnianski, C. P. 1967 Numerical computations of storm surges with bottom stress. *Mon. Weath. Rev. U.S. Dep. Agric.* **95**, 740–756.

Johns, B. & Ali, M. A. 1980 The numerical modelling of storm surges in the Bay of Bengal. *Q. Jl R. met. Soc.* **106**, 1–18.

Johns, B., Dube, S. K., Mohanty, U. C. & Sinha, P. C. 1981 Numerical simulation of the surge generated by the 1977 Andhra cyclone. *Q. Jl R. met. Soc.* **107**, 919–934.

Johns, B., Dube, S. K., Sinha, P. C., Mohanty, U. C. & Rao, A. D. 1982 The simulation of a continuously deforming lateral boundary in problems involving the shallow water equations. *Computers and Fluids* **10**, 105–116.

Johns, B., Sinha, P. C., Dube, S. K., Mohanty, U. C. & Rao, A. D. 1983*a* Simulation of storm surges using a three-dimensional numerical model: an application to the 1977 Andhra cyclone. *Q. Jl R. met. Soc.* **109**, 211–224.

Johns, B., Sinha, P. C., Dube, S. K., Mohanty, U. C. & Rao, A. D. 1983*b* On the effect of bathymetry in numerical storm surge simulation experiments. *Computers and Fluids* **11**, 161–174.

Miyazaki, M., Ueno, T. & Unoki, S. 1961 Theoretical investigations of typhoon surges along the Japanese coast. *Oceanogr. Mag.* **13**, 51–75.

Reid, R. O., Vastano, A. C., Whitaker, R. E. & Wanstrath, J. J. 1977 Experiments on storm surge simulation. In *The sea* (ed. E. D. Goldberg, I. N. McCave, J. J. O'Brien & J. H. Steele), vol. 6, pp. 145–168. New York: Wiley.

PHILOSOPHICAL TRANSACTIONS OF THE ROYAL SOCIETY A MATHEMATICAL, PHYSICAL & ENGINEERING SCIENCES